Fault-tolerant control of semi-active suspension in case of oil leakage of magnetorheological damper

Hakan Basargan and Filip Jeniš and András Mihály and Péter Gáspár

***Abstract*— The paper presents a reconfigurable fault-tolerant control strategy for a semi-active suspension using magnetorheological (MR) damper. The aim of the control reconfiguration is to handle the adverse behaviour of the MR damper due to oil leakage induced by the wear of the suspension component. The proposed method relies on the data driven model of the MR damper, using an estimation procedure to quantify the healthiness of the damper and to estimate the performance degradation due to the oil leakage. The reconfiguration control strategy is founded on the Linear Parameter Varying (LPV) framework, where a scheduling variable is defined to represent the healthiness level of the MR damper. By the scaling of the control action through the scheduling variable, the performance degradation of the MR damper can be compensated to match the behaviour of the healthy dampers. The proposed method is demonstrated through simulations, comparing the performance of the fault-tolerant LPV control to conventional semi-active control methods.**

I. Introduction

There are several damper types, such as monotube, twin-tube, internal-bypass, magneto-rheological(MR), spool-valve, and electronically controlled. MR damper appeared to be one of the most popular damper types for both academic and industrial projects that are related to suspension control. Compared with other dampers, MR dampers have great advantages such as stable hysteresis behavior, fast time response, and managing the balance between the objectives of the vehicle suspension control. Due to these advantages, an MR damper has been used in this study. The MR damper is a hydraulic device that has oil in it, and this oil contains metallic micro-sized particles that change the rheological properties of the MR fluid when a magnetic field is applied. The smart material of this damper presents changeable and functional properties and can be embedded in a damper actuator. The manipulation of the magnetic field is generated by applying an electric current through the damper coil. The damping ratio is modified by the variation of the oil viscosity [1].

Several studies have been presented in fault-tolerant semi-active suspension control. The study [2] introduces the design of a fault-tolerant semi-active suspension controller, while the fault-tolerant properties of the controller are realized by an LPV anti-windup approach using saturation indicator scheduling parameters. The paper [3] investigated the fault diagnosis and fault-tolerant methods of semi-active vehicle suspension system with MR damper to deal with the fault of MR damper. The research [4] introduces state-feedback fault-tolerant control with four modular fault estimation observers, while discussing seven approaches, analyzed and compared through realistic simulations to show the operation of each approaches. Paper [5] have used a neural network-based approach, and their fault isolation module is based on residual generation algorithms. The following study [6] proposed a fault-tolerant semi-active suspension control strategy with the LPV control method for the case when one of the dampers suffers from oil leakage. This control strategy calculates feasible damper forces for healthy dampers in order to compensate for the lost force of the faulty damper, while the operation of the proposed strategy is demonstrated in TruckSim simulation environment. The study [7] deals with a fail-safe MR damper that is resistant to power supply failure. The damper is equipped with a permanent magnet in the core, so in case of power supply failure, the damping force does not drop to a minimum and it is at least partially kept

Semi-active suspension systems have already been developed with different approaches. The Skyhook control [8], the linear-quadratic (LQ) control [9], mixed LTI $\mathcal{H}_\infty$ / $\mathcal{H}_2$ approaches [10], $\mathcal{H}_\infty$ control [11]. Thanks to the LPV framework, the controller can be modified with the external scheduling variable. This feature enables to modification of the controller online [12]–[17]. Due to this reason, the LPV framework has been used in this study in order to design a fault-tolerant controller for semi-active suspension. Present study introduces a reconfigurable fault-tolerant control strategy for a semi-active suspension equipped with an MR damper. The control reconfiguration aims to handle the oil leakage fault induced by the wear of the suspension component. The reconfiguration control strategy is founded on the LPV framework, where a scheduling variable is defined to represent the healthiness level of the MR damper. Another contribution of present article is using an MR damper in the LPV framework and designing the F-I converter that allows this use.

The paper is organized as follows: Section II contains

H. Basargan and P. Gáspár are with Department of Control for Transportation and Vehicle Systems, Budapest University of Technology and Economics, Stoczek u. 2, H-1111 Budapest, Hungary. E-mail: [hakan.basargan;gaspar.peter]@kjk.bme.hu

F. Jeniš is with Institute of Machine and Industrial Design, Faculty of Mechanical Engineering, Brno University of Technology, Technicka 2, 616 69 Brno, Czech Republic. E-mail: Filip.Jenis@vutbr.cz

A. Mihály and P. Gáspár are with Systems and Control Laboratory, Institute for Computer Science and Control (SZTAKI), Eötvös Loránd Research Network (ELKH), Kende u. 13-17, H-1111 Budapest, Hungary. E-mail: [mihaly.andras;gaspar.peter]@sztaki.hu

The research presented in this paper, carried out by Institute for Computer Science and Control was supported by the Ministry for Innovation and Technology and the National Research, Development and Innovation Office within the framework of the National Lab for Autonomous Systems. The research was further supported by Czech Science Foundation (GACR 21-45236L) and by the Brno University of Technology (FSI-S-23-8212).

MR damper modeling. Section III presents the quarter-car suspension model, F-I converter, and LPV controller design. Section IV demonstrates several simulation results where the proposed method is validated. Finally, concluding remarks are presented in Section V.

II. MR DAMPER MODEL

The model of the magnetorheological damper was created according to the real MR damper made and analyzed at the Brno University of Technology (Fig. 1). The magnetic circuit of this MR damper was made of Sintex SMC material to achieve a fast transient response. Thanks to this, the damper has excellent dynamic properties. A more detailed description of the damper is presented in the paper [18]. Inputs into

Fig. 1. MR damper during measurement

the damper model are electric current, and piston velocity and output is the damping force. To create a mathematical model of a damper, it was necessary to find its F-v-I map and its transient behaviour when the electric current changes.

A. F-v-I map

The F-v-I (force-velocity-electric current) map expresses the dependence of the damper force on the actual piston velocity and the electric current in the coil. The measurement of the F-v-I map was performed on the hydraulic pulsator, see Fig. 1. The logarithmic sweep with a constant amplitude of 20 mm was used as an excitation. The F-v-I map was calculated from measured data choosing the points with zero acceleration (centre of the stroke).

An important damper parameter affecting the effectiveness of semi-actively controlled damping is the dynamic force range [19] - the ratio of force in a fully activated and non-activated state. The dynamic force range of this damper is $dr = 7.6$ at piston velocity of $v = 0.1$ ms^{-1} (Fig. 2). The designed LPV controller requires quite different forces than the constructed damper shown in Fig. 1 has. However, changing the damper design enables to change its applicable forces while maintaining the same dynamic force range. Therefore, during the simulation, a damper with approximately half the forces compared to the measured ones was used (the

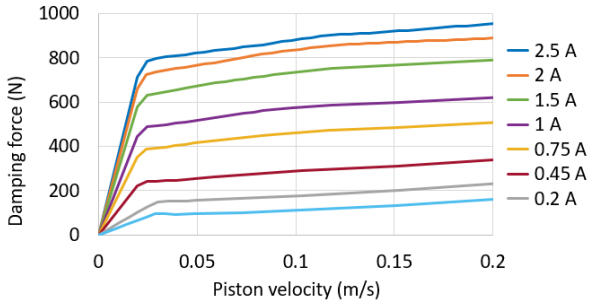

Fig. 2. F-v-I map of MR damper

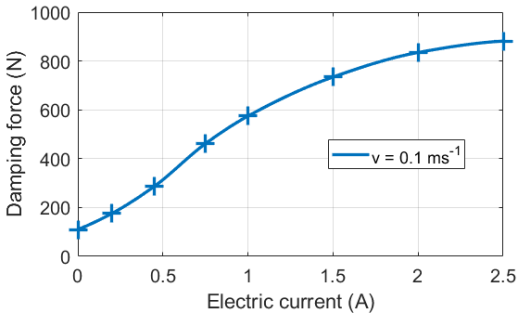

Fig. 3. Dependence of the damping force F_{mr} on the electric current I at a piston velocity of $v = 0.1$ ms^{-1}

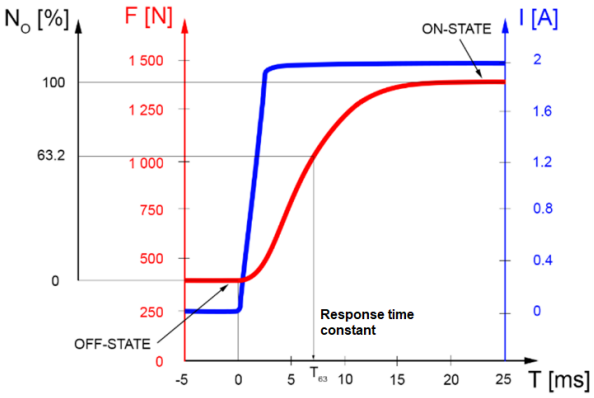

Fig. 4. Definition of damper response time constant τ_{63}

iteratively determined best setting). The applied F-v curves are shown in Fig. 2. The damper F-v curves are symmetrical for both tension and compression, whereas the graph shows only the positive F-v curves part.

Therefore, determining the damping force is easy when the damper piston velocity and electric current in the coil are known. For the actual piston velocity, the dependence of the damping force on the electric current is calculated by the Hermitian cubic polynomial at each step, for example, on the velocity of $v = 0.1$ ms^{-1} see Fig.3.

B. Transient behaviour

The transient behaviour of the MR damper can be described as a first-order system [20]. When the electric current

changes, the force course in a time can be described as follows:

$$F_i(v) = F_{i-1}(v) + (F_d(v) - F_{i-1}(v)) \cdot \left(1 - e^{-\frac{1}{\tau_{63} \cdot f_s}}\right) \quad (1)$$

where $F_i(v)$ is a force in the current step, $F_{i-1}(v)$ is a force in the previous step, $F_d(v)$ is a required force, v is a piston velocity, I is a electric current, τ_{63} is the response time constant, and f_s is sample frequency.

The constant τ_{63} represents the time in which the force reaches 63.2 % of the required force when the input signal (electric current) changes like unit-step [20], see Fig. 4. This time is possible to measure. The response time constant of the real damper was also measured using a hydraulic pulsator. The damper was tested without flexible silent blocks. The electric current was always activated in the middle of the damper stroke. The transient force response was measured for piston velocity of 0.1 ms^{-1} and electric current change from 0 A to 2 A. The methodology is described in more detail in [21]. The damper force response time constant was measured of τ_{63} = 1.8 ms. For simplicity, it will be considered the same value of the time constant for the force drop, but in reality, the force drop is slightly faster.

III. Semi-active suspension control

A. Vehicle model

The fault-tolerant system is designed in this study for a car represented by the two-degree-of-freedom quarter suspension model, see Fig. 5. Dynamic equations of the car model are following:

$$m_2\ddot{q_2} + k_2(q_2 - q_1) + F_{mr} = 0 \quad (2a)$$

$$m_1\ddot{q_1} + k_2(q_1 - q_2) + k_1(q_1 - w) - F_{mr} = 0 \quad (2b)$$

where m_2 and m_1 are the sprung and unsprung mass of the quarter vehicle, k_2 and k_1 are the stiffness of the spring and tire, and F_{mr} is the control force generated by the MR damper. Note that q_2 and q_1 are the vertical displacement of the sprung mass and the unsprung mass, while road disturbance is expressed with w. The parameters of the quarter model of a car suspension are shown in the Table I.

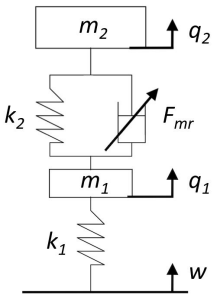

Fig. 5. Quarter-car model

TABLE I
SUSPENSION PARAMETERS

Parameter (symbol)	Value	Unit
sprung mass (m_2)	455	kg
unsprung mass (m_1)	50	kg
suspension stiffness (k_2)	25	kNm^{-1}
tire stiffness (k_1)	120	kNm^{-1}

B. Controller design

An LPV framework has been used in order to design a fault-tolerant controller for semi-active suspension. The LPV performance problem is to choose a parameter-varying controller, which guarantees quadratic stability for the closed-loop system while the induced $\mathcal{L}_2$ norm from the disturbance ω to the performances z is smaller than the value γ, as described in [22]. Therewith, the minimization task is given as:

$$\inf_K \sup_{\varrho \in \mathcal{F}_\mathcal{P}} \sup_{\|w\|_2 \neq 0, w \in \mathcal{L}_2} \frac{\|z\|_2}{\|w\|_2} \leq \gamma. \quad (3)$$

The solution of an LPV problem is directed by the set of infinite-dimensional LMIs being satisfied for all $\rho \in \mathcal{F}_\mathcal{P}$, thus it is a convex problem. In practice, this problem is set up by gridding the parameter space and solving the set of LMIs that hold on the subset of $\mathcal{F}_\mathcal{P}$, see [23]. The existence of a controller that solves the quadratic LPV γ-performance problem can be expressed as the feasibility of a set of LMIs that can be solved numerically. The proof of the existence of the solution is available in study of [24].

The state vector is $x = [x_1, x_2, x_3, x_4]$, in which the components are $x_1 = q_2$, $x_2 = \dot{q_2}$, $x_3 = q_1$, $x_4 = \dot{q_1}$. The performance is defined as passenger comfort described by sprung mass velocity, with the following optimization criterion: $z = \dot{q_2} \to 0$. In the design, the measured signal is also chosen as sprung mass velocity $\dot{q_2}$. The control input u is the theoretical ideal control force. This force u operates as an input to the F-I (force $\to$ current) converter required for the MR damper model. The unmodelled dynamics Δ are considered with Δ = 0.2.

The system given with dynamic equations (2) is transformed into the state-space representation form as an equation (4).

$$\begin{bmatrix} \dot{x_1} \\ \dot{x_2} \\ \dot{x_3} \\ \dot{x_4} \\ z \end{bmatrix} = \begin{bmatrix} 0 & 1 & 0 & 0 & 0 & 0 \\ -\frac{k_2}{m_2} & 0 & \frac{k_2}{m_2} & 0 & 0 & \frac{1}{m_2} \\ 0 & 0 & 0 & 1 & 0 & 0 \\ \frac{k_2}{m1} & 0 & -\frac{k_2+k_1}{m_2} & 0 & \frac{k_1}{k_2} & -\frac{1}{m_1} \\ 0 & 1 & 0 & 0 & 0 & 0 \end{bmatrix} \begin{bmatrix} x_1 \\ x_2 \\ x_3 \\ x_4 \\ w \\ u \end{bmatrix} \quad (4)$$

The introduced controller is founded on a closed-loop architecture shown in Fig. 6. In the interconnection structure, G is the quarter-car model defined in (2), K is the designed LPV controller characterized with the scheduling variable ρ responsible for control reconfiguration, u defines the control input, y represents the measured output, n expresses the

measurement noise, z represents the performance output, and w stands for the road disturbance.

The weighting functions W_n and W_d represent sensor noise and road disturbances, while W_r stands for the parameter uncertainties. The weighting function W_p is to keep the sprung mass velocity small. Note, that the weighting functions W_n, W_d, W_r and W_p are all in linear form without containing the scheduling variable ρ. The weighting function W_u, which is responsible for the fault configuration, will be described in the next section.

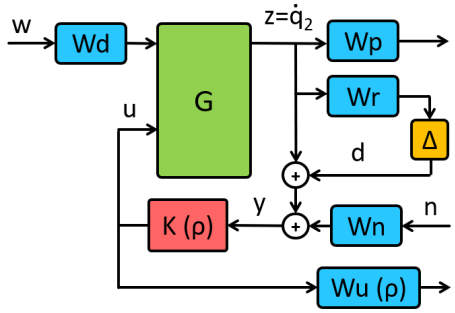

Fig. 6. Closed-loop interconnection structure

C. F-I converter

Two problems hinder the implementation of the MR damper mathematical model into the suspension system: 1) the output from the controller is a force, but the input to the MR damper model is an electric current, 2) the MR damper is able to create forces only in the interval $[F_{min}, F_{max}]$ for a specified piston velocity when F_{min} corresponds to a current of 0 A and F_{max} to a current of 2.5 A.

The F-I converter solves these two problems. First, the realizable damper force is calculated according to the equation:

$$F_r(v,u) = \begin{cases} F_{max}(v), & \text{if } u > F_{max}(v) \\ u, & \text{if } F_{min}(v) < u < F_{max}(v) \\ F_{min}(v), & \text{if } u < F_{min}(v) \end{cases} \tag{5}$$

where $F_r(v,u)$ is the realizable damping force, $F_{max}(v)$ and $F_{min}(v)$ are maximal and minimal damping forces for specified piston velocity, v is piston velocity, and u is the ideal damping force from the controller.

The second task is to convert the force F_r to the electric current value I. Knowing piston velocity and F-v-I map, interpolation by a Hermitian cubic polynomial is used for it, the same as in the case of the MR damper model, see Fig. 3.

D. Fault-tolerant control configuration method

The model of oil leakage fault, which induces a decrease of force in MR damper is written as follows:

$$F_{mrf} = \phi \cdot F_{mr} \tag{6}$$

where F_{mrf} is the faulty damper force (real damping force), F_{mr} is the assumed damper force, and $\phi \in (0,1]$ is the degree of oil leakage.

The effort of the fault-tolerant system is to increase the value of the electric current in the damper coil when the difference between the real damping force and the assumed damping force is founded and thus compensate for this force loss. This can be achieved by changing the weight function W_u, which is responsible for the value of the damping force. Thus this function is defined as follows:

$$W_u = \rho \cdot w_u \tag{7}$$

where W_u is the weighting function for control force u, ρ is a scheduling variable, and w_u is the control weighting function used in the case of the non-faulty damper ($\phi = 1$, $\rho = 1$). The scheduling variable ρ lies in the interval $(0,1]$. The case without fault corresponds to $\rho = 1$, and as the fault increases, ρ decreases. It is necessary to define the compensation constant κ, which determines the dependence of the compensation amount on the fault level. Therefore, ρ is defined as follows:

$$\rho = 1 - (1 - F_{mrf}/F_{mr}) \cdot \kappa \tag{8}$$

where F_{mrf} is the faulty damper force (from a model of oil leakage fault, it will be measured in practice), F_{mr} is the assumed damper force (from a model of non-faulty damper), and κ is a compensation constant. Values of w_u, W_p and κ were iteratively found. The criterion for optimizing these parameters was the minimum RMS of the sprung mass acceleration ($\ddot{q}_2$) in fault-free and fault-compensated cases.

IV. Results

The simulations were performed in Matlab/Simulink. The simulation architecture is shown in Fig. 7. The sinusoidal sweep was used for the excitation of a car suspension, see Fig. 8. This kind of road irregularity is typical at bus stops, where the frequent braking of heavy road vehicles rolls up the asphalt.

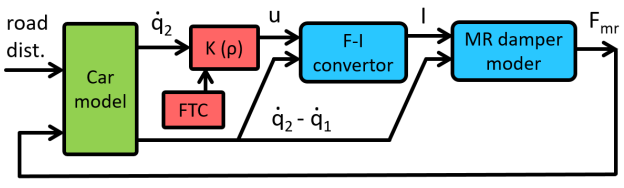

Fig. 7. Architecture of simulations

First, LPV performance was compared with Skyhook and passive performance, see Fig. 9. Skyhook is one of the simplest semi-active suspension algorithms focused on comfort, described in [8]. For the passive damping case, a permanent electric current was necessary to choose besides the damper scale. Current I = 1 A was chosen as the best case for passive damping. RMS of sprung mass acceleration is 0.443 ms^{-2} when LPV control is used, 0.477 ms^{-2} when Skyhook control is used, and 0.650 using a passive damper.

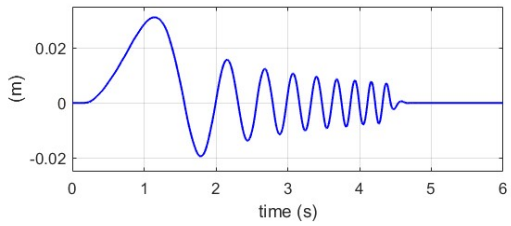

Fig. 8. Road disturbance w

Thus improvement of LPV compared to passive is 32 %, and 27 % of Shyhook compared to passive.

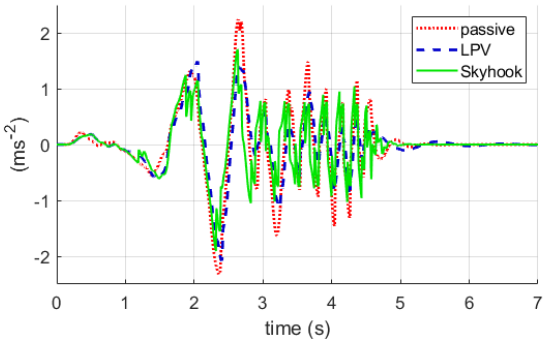

Fig. 9. Comparison of sprung mass acceleration for LPV control and Skyhook algorithm

Three scenarios were simulated in order to demonstrate the effectiveness of the proposed fault-tolerant system:

- Fault-free
- Fault ϕ = 0.5, uncompensated
- Fault ϕ = 0.5, compensated

The following quantities in simulations were evaluated:

- Acceleration of sprung mass $\ddot{q}_2$
- Velocity of sprung mass $\dot{q}_2$
- Displacement of sprung mass q_2

In addition, the following quantities are also monitored:

- Damping force F_{mr}
- Damper state (0 % - 100 %)

Table II shows the results of RMS of evaluated quantities for simulated cases, also the improvement of the compensated case compared to the uncompensated case is shown. It can be seen that the RMS of the sprung mass acceleration was decreased by 14 % when compensating for the fault compared to the uncompensated case, and the velocity RMS was decreased even by 18 %. For the displacement, it is reduced by 11 %.

Figures 10-12 show course of evaluated quantities: $\ddot{q}_2$, $\dot{q}_2$ and q_2. It can be seen that the course of the dynamic quantities of the sprung mass when compensating for the fault of ϕ = 0.5, is almost identical to the course of the quantities with the fully functional damper. Thus it can be stated that the designed fault-tolerant system operates well.

Figures 13 and 14 show the damper state and damping force. State 1 means damping force F_{max}, 0 represents F_{min},

TABLE II

RMS OF EVALUATED QUANTITIES

Quantity (unit)	Fault free	Fault ϕ = 0.5	Fault comp.	Improvement
$\ddot{q}_2$ (ms^{-2})	0.443	0.509	0.440	14 %
$\dot{q}_2(ms^{-1})$	0.054	0.068	0.056	18 %
$q_2(ms)$	0.011	0.013	0.011	11 %

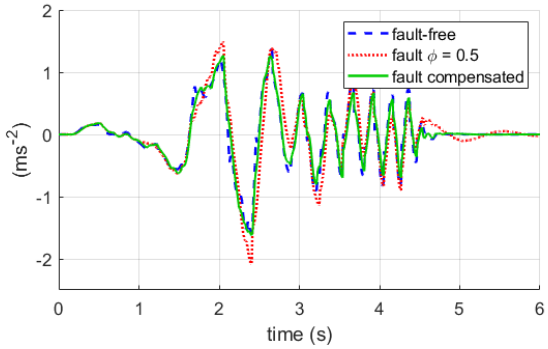

Fig. 10. Acceleration of sprung mass $\ddot{q}_2$

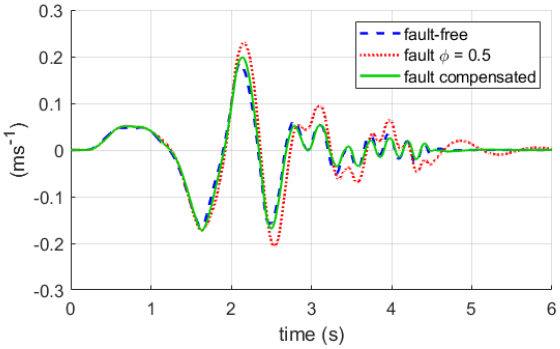

Fig. 11. Velocity of sprung mass $\dot{q}_2$

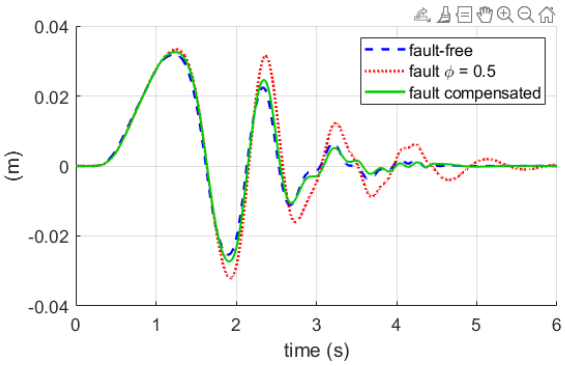

Fig. 12. Displacement of sprung mass q_2

and 0.5 belongs to $(F_{max} + F_{min})/2$ for the relevant case. It can be seen that when compensating for the fault, the damper uses more of the maximum currently possible force. When compensating for the fault, the effort is to increase the damping force, hence it is necessary to increase the value of the electric current in the coil. However, it is not possible

to increase the current over 2.5 A. Thus the force cannot exceed F_{max} for the relevant damper case.

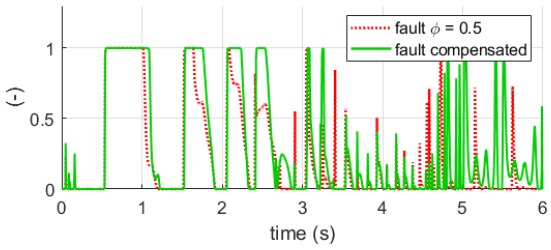

Fig. 13. Damper state

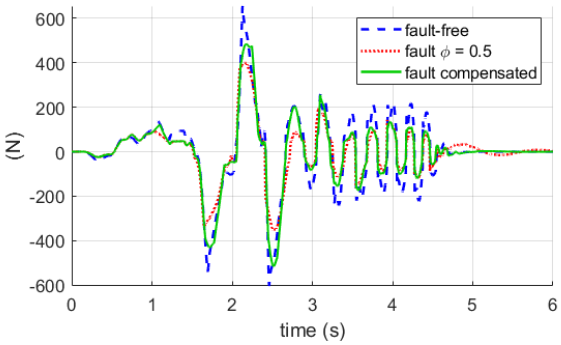

Fig. 14. Damping force F_{mr}

V. Conclusion

The paper proposed the design of semi-active suspension control with fault-tolerant reconfiguration through the LPV control framework. The fault-tolerant control strategy aims to compensate for the MR damper fault effects. The proposed method calculates a feasible compensated damper force for the faulty dampers in case of performance degradation induced by oil leakage. Several simulations had been performed in order to demonstrate the operation of the proposed method. First, the designed reconfigurable LPV controller was compared with Skyhook and passive suspension. Then, simulations were evaluated with healthy and faulty semi-active suspensions along with the proposed compensated fault-tolerant design. Simulation results proved that the designed fault-tolerant semi-active suspension controller improved the performance of the vehicle.

References

[1] J. de Jesus Lozoya-Santos, J. C. Tudón-Martinez, R. Morales-Menendez, R. Ramirez-Mendoza, and L. E. Garza-Castanon, "A fault detection method for an automotive magneto-rheological damper," *IFAC Proceedings Volumes*, vol. 45, no. 20, pp. 1209 – 1214, 2012, 8th IFAC Symposium on Fault Detection, Supervision and Safety of Technical Processes.

[2] M. Fleps-Dezasse, F. Svaricek, and J. Brembeck, "Damper fault-tolerant linear parameter-varying semi-active suspension control," *IFAC-PapersOnLine*, vol. 50, no. 1, pp. 8592 – 8599, 2017.

[3] X. Du, G. Han, M. Yu, Y. Peng, X. Xu, and J. Fu, "Fault detection and fault tolerant control of vehicle semi-active suspension system with magneto-rheological damper," *Smart Materials and Structures*, vol. 30, no. 1, p. 014004, 2020.

[4] M. M. Morato, O. Sename, and L. Dugard, "Design and analysis of several state-feedback fault-tolerant control strategies for semi-active suspensions," *IFAC-PapersOnLine*, vol. 52, no. 17, pp. 48–53, 2019.

[5] S. A. Rueda Villanoba and C. Borrás Pinilla, "Neural network based fault tolerant control for a semi-active suspension," in *ASME International Mechanical Engineering Congress and Exposition*, vol. 59414. American Society of Mechanical Engineers, 2019, p. V004T05A089.

[6] H. Basargan, A. Mihály, P. Gáspár, and O. Sename, "Fault-tolerant semi-active suspension control for degradation in damper performance," in *2021 29th Mediterranean Conference on Control and Automation (MED)*. IEEE, 2021, pp. 1191–1196.

[7] F. Jeniš, M. Kubík, O. Macháček, and Z. Šebesta, K andStrecker, "Insight into the response time of fail-safe magnetorheological damper," *Smart Materials and Structures*, vol. 30, no. 1, 2021.

[8] C. Liu, L. Chen, X. Yang, X. Zhang, and Y. Yang, "General theory of skyhook control and its application to semi-active suspension control strategy design," *IEEE Access*, vol. 7, pp. 101 552–101 560, 2019.

[9] J. A. Genov and I. M. Kralov, "A linear quadratic regulator synthesis for a semi-active vehicle suspension part 2–multi-objective synthesis," in *AIP Conference Proceedings*, vol. 2172, no. 1. AIP Publishing LLC, 2019, p. 110007.

[10] S. M. Badran, "Robust lmi-based controller design using hinf and mixed h2/hinf for semi active suspension system," *Editorial Committees*, vol. 2, no. 8, pp. 172–180, 2012.

[11] A. Zin, O. Sename, and L. Dugard, "Switched h_{inf} control strategy of automotive active suspensions," *Proceedings of the 16th IFAC world congress (WC), Praha, Czech Republic*, pp. 198–203, 2005.

[12] H. Basargan, A. Mihály, Á. Kisari, P. Gáspár, and O. Sename, "Vehicle semi-active suspension control with cloud-based road information," *Periodica Polytechnica Transportation Engineering*, vol. 49, no. 3, pp. 242–249, 2021.

[13] H. Basargan, A. Mihály, P. Gáspár, and O. Sename, "Road adaptive semi-active suspension and cruise control through lpv technique," in *2021 European Control Conference (ECC)*. IEEE, 2021, pp. 461–466.

[14] H. Basargan, A. Mihály, P. Gáspár, and O. Sename, "Integrated multi-criteria velocity and semi-active suspension control based on look-ahead road information," in *2020 28th Mediterranean Conference on Control and Automation (MED)*. IEEE, 2020, pp. 25–30.

[15] H. Basargan, A. Mihály, P. Gáspár, and O. Sename, "Adaptive semi-active suspension and cruise control through lpv technique," *Applied Sciences*, vol. 11, no. 1, 2021. [Online]. Available: https://www.mdpi.com/2076-3417/11/1/290

[16] H. Basargan, A. Mihály, P. Gáspár, and O. Sename, "An lpv-based online reconfigurable adaptive semi-active suspension control with mr damper," *Energies*, vol. 15, no. 10, p. 3648, 2022.

[17] H. Basargan, A. Mihály, P. Gáspár, and O. Sename, "Integrated adaptive velocity and semi-active suspension control for different road profiles," in *2022 30th Mediterranean Conference on Control and Automation (MED)*. IEEE, 2022, pp. 933–938.

[18] Z. Strecker, F. Jeniš, M. Kubík, O. Macháček, and S. B. Choi, "Novel approaches to the design of an ultra-fast magnetorheological valve for semi-active control," *Materials*, vol. 14, no. 10, 2021.

[19] O. Macháček, M. Kubík, Z. Strecker, J. Roupec, and I. Mazůrek, "Design of a frictionless magnetorheological damper with a high dynamic force range," *Advances in Mechanical Engineering*, vol. 11, no. 3, 2019.

[20] F. D. Goncalves, J. H. Koo, and M. Ahmadian, "Experimental approach for finding the response time of mr dampers for vehicle applications," in *Proceedings of the ASME Design Engineering Technical Conference*, 2003, pp. 425–430.

[21] Z. Strecker, J. Roupec, I. Mazurek, O. Machacek, M. Kubik, and M. Klapka, "Design of magnetorheological damper with short time response," *Journal of Intelligent Material Systems and Structures*, vol. 26, no. 14, pp. 1951–1958, 2015.

[22] J. Bokor and G. Balas, "Linear parameter varying systems: A geometric theory and applications," *16th IFAC World Congress, Prague*, 2005.

[23] F. Wu, X. H. Yang, A. Packard, and G. Becker, "Induced l^2-norm control for LPV systems with bounded parameter variation rates," *International Journal of Nonlinear and Robust Control*, vol. 6, pp. 983–998, 1996.

[24] J. Yu and A. Sideris, "Hinf control with parametric lyapunov functions," *Systems & Control Letters*, vol. 30, no. 2-3, pp. 57–69, 1997.